DOI: 10.1002/chem.200801399

Influence of Endohedral Confinement on the Electronic Interaction between He atoms: A $He_2@C_{20}H_{20}$ Case Study

Erick Cerpa,[a] Andreas Krapp,[b] Roberto Flores-Moreno,[a] Kelling J. Donald,[c] and Gabriel Merino*[a]

Abstract: The electronic interaction between confined pairs of He atoms in the $C_{20}H_{20}$ dodecahedrane cage is analyzed. The He–He distance is only 1.265 Å, a separation that is less than half the He–He distance in the free He dimer. The energy difference between the possible isomers is negligible (less than 0.15 kcal mol^{-1}), illustrating that there is a nearly free precession movement of the He_2 fragment around its midpoint in the cage. We consider that a study of inclusion complexes, such as the case we have selected and other systems that involve artificially compressed molecular fragments, are useful reference points in testing and extending our understanding of the bonding capabilities of otherwise unreactive or unstable species. A key observation about bonding that emerges uniquely from endohedral (confinement) complexes is that a short internuclear separation does not necessarily imply the existence of a chemical bond.

Keywords: Bader theory · bond theory · density functional calculations · endohedral confinement · energy decomposition analysis

Theoretical interest in the nature of small helium clusters dates back at least to Slater some eighty years ago.[1] However, definitive experimental evidence for the existence of the helium dimer became available only in last two decades.[2,3] The potential-energy curve of the He_2 unit is repulsive, except for a very shallow van der Waals minimum. Coupled cluster calculations give a dissociation energy of only $D_e = 0.021$ kcal mol^{-1}.[4] As pointed out recently in reference [5], this is 5000 times smaller than D_e for the covalent H_2 bond.

The molecular orbital explanation for the non-existence of a covalently bonded He_2 is well described in general chemistry texts. He_2 is a simple case of a two-orbital four-electron interaction in which the filling of both the bonding σ_g and antibonding σ_u* molecular orbitals (MOs) results in a net repulsion between the two He centers. An evident strategy for enhancing the bonding between the two He centers is, therefore, removal of electrons from the σ_u* orbital. The brute-force electron-stripping method in which one or both electrons are completely removed from the antibonding MO, for example, has been employed. The result is a significant stabilization: while He_2 is a weak dimer with a large vibrational amplitude, the electronic ground state of He_2^+ is more strongly bound.[6,7] Shifting some of the charge density out of the He_2 HOMO into the bonding LUMO is a chemically more interesting way of reducing the σ_u* orbital population, but the LUMO is quite high in energy.

Although the He_2 dimer is not a particularly stable unit, carbon cages containing one or two He atoms trapped at "unnaturally" close interatomic separations have been studied both experimentally and computationally. For instance, several endohedral complexes containing two noble gas atoms have been synthesized by Saunders and co-workers.[8–10] More recently, Krapp and Frenking carried out a computational study of the endohedral fullerene complexes $Ng_2@C_{60}$ (Ng = He, Ne, Ar, Kr and Xe).[11] They found that a precession movement of He_2 in the C_{60} cage has practically no barrier, with a He–He distance in $He_2@C_{60}$ (1.948 Å) far shorter than that in the free He_2 dimer (2.977 Å).[4,11] Krapp and Frenking also determined that all five of the $Ng_2@C_{60}$

[a] E. Cerpa, Dr. R. Flores-Moreno, Prof. G. Merino
Facultad de Química. Universidad de Guanajuato
Noria Alta s/n CP 36050, Guanajuato, Gto. (México)
Fax: (+52) 473-732-0006/-8120
E-mail: gmerino@quijote.ugto.mx

[b] Dr. A. Krapp
Senter for teoretisk og beregningsorientert kjemi
Kjemisk institutt, Universitetet i Oslo
Postboks 1033 Blindern, 0315 Oslo (Norway)

[c] Dr. K. J. Donald
Department of Chemistry
Gottwald Center for the Sciences, University of Richmond
Richmond, Virginia 23173 (USA)

complexes they considered are thermodynamically unstable towards the reactants (the free C_{60} and two Ng atoms).

Despite the very short He–He interatomic separation (1.948 Å) obtained for the $He_2@C_{60}$ complex, Krapp and Frenking concluded that there is no bonding between the He centers. Evidence of bonding was found, however, between the pair of Xe atoms that were similarly trapped in a C_{60} cage. Since the atomic radius of the Xe atoms is significantly larger than that of the He atoms, and the ionization of Xe is relatively low, trapping a pair of Xe atoms in the C_{60} cage ensures far more significant Xe–Xe and C–Xe interactions compared to the helium case (and the cases of the other Ng atoms smaller than Xe). The minimum energy $Xe_2@C_{60}$ structure they obtained exhibited clear evidence of bonding between the two included Xe atoms, accompanied by a significant transfer of charge density from the Xe–Xe antibonding molecular orbital onto the C_{60} cage.

A question we ask in this paper is whether a similar *chemical confinement* strategy, which employs a significantly smaller cage to ensure shorter He–cage and He–He contacts, may be sufficient to realize bonding between the helium centers? For this purpose we consider the theoretical $He_2@C_{20}H_{20}$ system in which the two helium atoms are confined in the $C_{20}H_{20}$ cage. Beyond an interest in the electronic properties of $Ng_2@$Cage systems, we want to assess, as well, the influence of structural compression and confinement on chemical bonding.

Geometries and energies: Three unique isomers of the $He_2@C_{20}H_{20}$ complex optimized under symmetry constraints are shown in Figure 1. Frequency analysis shows that all of them are local minima. In the D_{2h} structure, the He–He axis is oriented along the line connecting the midpoints of two opposing C–C bonds in the cage (Figure 1). In the other two isomers the helium dimer is oriented 1) along the axis between two opposing carbon atoms (the D_{3d} structure), and 2) along the axis between the midpoints of two opposing five-membered rings of the cage (the D_{5d} structure).

Note that all of the isomers are essentially identical energetically (all of the isomers are within 0.15 kcal mol^{-1} of each other), indicating that there is a nearly free precession movement of the He_2 fragment around its midpoint in the cage. So, the symmetry assignment for a frozen equilibrium structure is not relevant at room temperature.

The trapped He–He pair has an internuclear separation of 1.265 Å! At the RI-MP2 level this separation is almost identical (1.263 Å), and is some 1.71 Å shorter than the computed minimum-energy distance obtained for the uncompressed helium van der Waals dimer (2.977 Å).[4] Indeed, the endohedral He–He interatomic separation we have obtained is the shortest reported so far; but it comes at a cost: in the case of the D_{2h} structure (Figure 2), the C–C bonds oriented along the He–He axis are elongated from 1.551 to 1.618 Å. Overall the cage expands along the He–He axis from 4.062 Å in the free $C_{20}H_{20}$ to 4.301 Å.

The difference between the sum of the van der Waals radii of two carbon atoms (≈3.4 Å)—one C atom each from opposite sides of the expanded cage—and the diameter of the cage (≈4.3 Å) is only 0.9 Å; a tight spot in which to squeeze two He atoms. In the minimum-energy structure, the He–He separation (1.265 Å; vide supra) is larger than 0.9 Å, implying that there is a significant He–C (van der Waals) interpenetration. The evident difficulty of getting two He atoms into this restrictive space may explain why only the complex with one He atom in a $C_{20}H_{20}$ cage ($He@C_{20}H_{20}$) has been synthesized so far.[12,13]

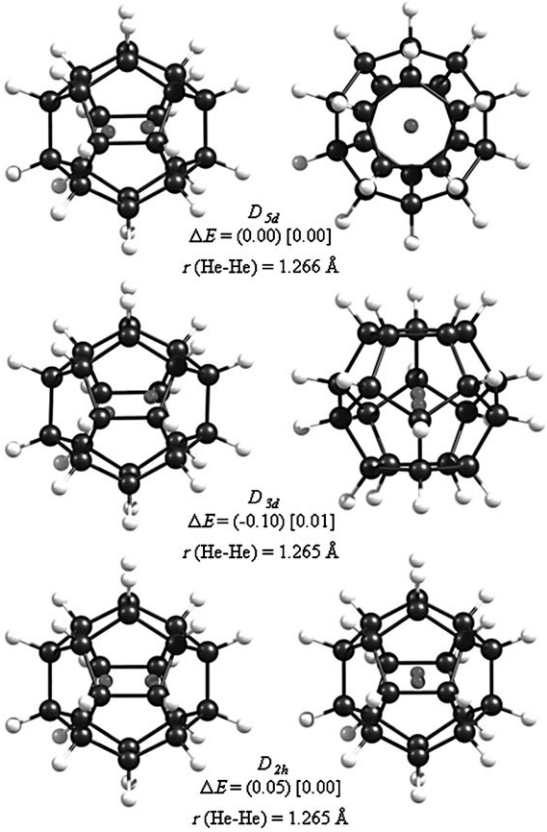

Figure 1. Isomers of $He_2@C_{20}H_{20}$ optimized at the B3LYP/def2-TZVPP[32–34] and the RI-MP2/def2-TZVPP[34–36] levels, using the Turbomole suite of programs.[37] The relative energies (with respect to the D_{5d} structure) obtained from the B3LYP and RI-MP2 calculations are given in kcal mol^{-1} units in round and square brackets respectively.

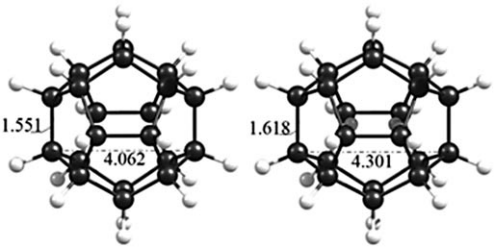

Figure 2. Computed (B3LYP/def2-TZVPP) geometry of $C_{20}H_{20}$ and $He_2@C_{20}H_{20}$ (D_{2h}). Key interatomic separations are given in Å.

Dissociation energies and the energy decomposition analysis: The highly repulsive nature of the He–He and He_2–$C_{20}H_{20}$ interactions is evident in the dissociation energy D_e for $He_2@C_{20}H_{20}$ going to the He atoms and the free $C_{20}H_{20}$ cage [Eq. (1); see also Table 1].

$$He_2@C_{20}H_{20} \rightarrow He_2+C_{20}H_{20} \quad (1)$$

Table 1. Dissociation energies (D_e), interaction energies (E_{int}), counterpoise corrected interaction energies[14] ($E_{int,BSSE}$), and preparation energies (E_{prep}) for D_{2h} $He_2@C_{20}H_{20}$. All values in kcal mol^{-1}.

	B3LYP/def2-TZVPP	RI-MP2/def2-TZVPP
D_e	−169.8	−157.5
E_{int}	124.9	111.8
$E_{int,BSSE}$	125.8	115.0
$E_{prep}(C_{20}H_{20})$	14.5	14.2
$E_{prep}(He_2)$	30.4	31.5

For $He_2@C_{20}H_{20}$, the dissociation energy as defined above at the MP2 and B3LYP levels are $D_e = -157.4$ kcal mol^{-1} and -169.8 kcal mol^{-1}, respectively. To gain a bit more insight into the energetics, we separated the dissociation energy into two contributions: $-D_e = E_{int} + E_{prep}$. The interaction energy (E_{int}) gives the repulsive contribution between the geometrically deformed $C_{20}H_{20}$ and the He_2 dimer with a He–He distance as in the complex. The preparation energy (E_{prep}) is the energy needed to deform the cage and to bring the He atoms closely together. It is clear from Table 1 that the overall interaction between the cage and the two He atoms is repulsive ($E_{int} = 111.8$ kcal mol^{-1} at the MP2 level) and is the dominant contribution to the overall dissociation energy. The total energy required to deform the cage is relatively small (14.2 kcal mol^{-1} at MP2), and is the net result of several geometrical (bond length and angular) modifications in the $C_{20}H_{20}$ skeleton. Forcing the He atoms closer together costs roughly twice as much in energy (31.5 kcal mol^{-1}).

We also employed an energy decomposition analysis (EDA)[15–17] to estimate the strength of the individual contributions to the total electronic energy of the $He_2@C_{20}H_{20}$ complex. The EDA was carried out by using He_2 and $C_{20}H_{20}$ as fragments. From the EDA results, it becomes evident that the repulsive interactions between the He_2 fragment and the cage come from the Pauli repulsion (See Table 2). Both the orbital and electrostatic contributions (ΔE_{orb} and ΔE_{elstat}, respectively) are attractive. The largest attractive contribution comes from the electrostatic term ($\Delta E_{elstat} = -77.6$ kcal mol^{-1}). This value is much higher than those calculated for $He_2@C_{60}$ (-3.5 kcal mol^{-1}), indicating a strong electrostatic attraction between both fragments.

Table 2. Results of the EDA at BP86[18,19]/TZ2P//B3LYP/def2-TZVPP for the D_{2h} structure of $He_2@C_{20}H_{20}$ by using He_2 and $C_{20}H_{20}$ as fragments. Energy values kcal mol^{-1}.

ΔE_{int}	122.1	ΔE_{pauli}	241.3
ΔE_{elstat}	−77.6	ΔE_{orb}	−41.6
a_g	−17.4	b_{1g}	−1.0
b_{2g}	−0.2	b_{3g}	−1.0
a_u	−0.1	b_{1u}	−1.7
b_{2u}	−18.4	b_{3u}	−1.8

The partition of the orbital term into contributions of the orbitals belonging to different irreducible representations of the point group shows that the a_g term, which contains the He–He σ-bonding and He_2-$C_{20}H_{20}$ attractive interactions, has nearly the same strength as the b_{2u} term.

Charge distribution: The discovery and analysis of unusual molecular motifs, such as the endohedral complexes considered in this paper, (described as artificial in references [8,10]) often compel chemists to reexamine our understanding of that inherently fuzzy concept we call the chemical bond. For the $Ng_2@C_{60}$ endohedral complexes, such a reevaluation has been carried out by one of us and Frenking in a recent study.[7]

In this section we move directly into an assessment of the charge distribution in the title $He_2@C_{20}H_{20}$ system using different—but by now conventional—methods for describing the charge distribution in molecules: the topological analysis due to Bader et al.,[20] the natural population analysis, and Wiberg bond indices.[21]

Bader analysis: We start by using the topological analysis of the electron density following Bader's atoms in molecules analysis.[20] Bader pointed out in reference [22] that if two fragments interact strongly within a molecular system, then the electron density will exhibit a saddle point in the region between the nuclei, and the nuclei will be linked by a bond path. In Figure 3, the molecular graphs of the three isomers

Figure 3. Molecular graphs for different isomers of $He_2@C_{20}H_{20}$. A (3,−1) critical point is denoted by the smallest spheres.

obtained by using the AIM2000 program[23,24] are shown, employing the wave functions obtained in Gaussian 98.[25] The analysis identifies a He–He bond path and a He–C bond path for each He atom for the D_{3d} structure, suggesting that each helium atom is dicoordinated. However, the bonding scenario drastically changes for the D_{5d} and D_{2h} structures, for which the Bader analysis indicates pentacoordination and tricoordination for each helium atom, respectively. A recent analysis by some of the present authors confirms that the number of bond paths obtained between atoms in molecular cages and the atoms in the cage framework is a function of the molecular symmetry,[26] and is not necessarily indicative of the presence of a chemical bond be-

tween atoms. It is hardly straightforward, therefore, to tell whether a computed bond path denotes the presence of a real bond or is simply an artifact of the topological analysis.[27–30]

Further, the Laplacian ($\nabla^2\rho(\mathbf{r})$) map (Figure 4) shows that this scalar field is positive (solid lines) over the entire region of the He–He and He–C interactions, with a tiny distortion

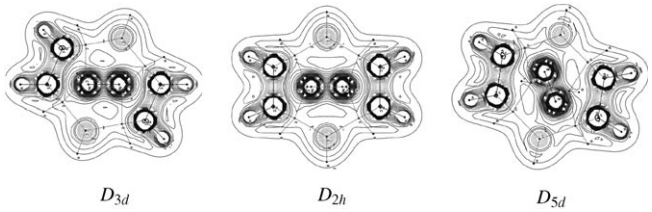

Figure 4. Contour line map of $\nabla^2\rho(\mathbf{r})$. Dashed lines indicate areas of charge concentration ($N^2\rho(\mathbf{r})<0$). Solid lines indicate areas of charge depletion ($\nabla^2\rho(\mathbf{r})>0$).

in the charge depletion area along the connecting path between the helium atoms, suggesting that the He–X (X = C, He) interactions result from the contact of closed-shell fragments. The properties of $\rho(\mathbf{r})$ at the associated (3,−1) critical points reflect key characteristics associated with weak intermolecular interactions: a low value for $\rho_{\text{He-X}}$ and $\nabla^2\rho(\mathbf{r})>0$ (Figure 4).

In contrast, the calculated $\rho_{\text{C–C}}$ and the negative values of the Laplacian at the (3,−1) critical points associated with the C–C bonds are usual for covalent bonds (See Figure 4, dashed lines indicate that $\nabla^2\rho(\mathbf{r})<0$). Our conclusion that the occurrence of a bond path between the He centers is not evidence for the existence of a covalent bond between the two He atoms is supported strongly by the charge density data. Note that the $\rho_{\text{He–He}}$ value in the $He_2@C_{20}H_{20}$ ($\rho_{\text{He–He}}=0.101$ a.u.) is only slightly higher than that reported for the $He_2@C_{60}$ complex in reference [11] ($\rho_{\text{He–He}}=0.094$ a.u.), despite a significant shortening of the He–He separation by 0.5 Å going from $He_2@C_{60}$ cage to $He_2@C_{20}H_{20}$.

Natural population analysis and Wiberg indexes: [21,31] Given that the ionization energy of the He atom itself is rather high (compared to the heavier noble gas atoms) and the electron affinity of $C_{20}H_{20}$ is low, it is expected that any electronic transfer from the He atoms to the cage will be small. Indeed, a natural population analysis on the $He_2@C_{20}H_{20}$ complex gives an insignificant charge separation of +0.05 on the helium atom (Table 1). This indicates that the He_2 fragment donates effectively no charge density to the $C_{20}H_{20}$ cage. In fact, although the He–He bond length is significantly shorter in the cage than it is in the free He_2, the calculated values of He–He Wiberg bond index[21] show that the He–He bond order is zero. We obtain no noticeable charge transfer between the two He atoms in the cage. This is in contrast to the $Xe_2@C_{60}$ case, for instance, in which a charge for Xe of +1.06 was obtained.[11] Negligible Wiberg bond indices of 0.015 are also obtained for the He–C contacts, indicative of the inert nature of He even in comparison to the other noble gas atoms (for which some bonding is evident in C_{60}) and despite the shorter interatomic separation with the neighboring atoms in the $C_{20}H_{20}$ cage.

Molecular orbital analysis: Figure 5 shows the contour maps of the most important molecular orbitals involving the helium atoms. The HOMO energy for the isolated He_2

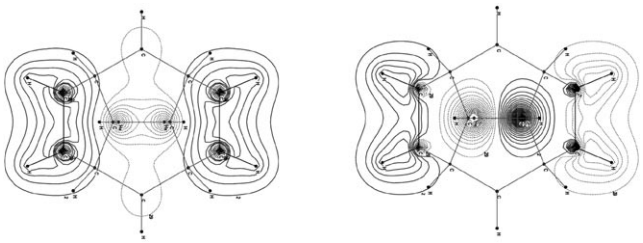

Figure 5. The contour maps of the relevant molecular orbitals involved in the He–He interaction for the D_{2h} $He_2@C_{20}H_{20}$ structure calculated at the B3LYP/def2-TZVPP level.

dimer with the He–He distance in $He_2@C_{20}H_{20}$ is −17.75 eV (at the B3LYP level). Note that the HOMO of the free He_2 is mixed into a b_{3u} orbital (−16.71 eV) for the $He_2@C_{20}H_{20}$ complex.

The change in the energy level going from the free He_2 to the $He_2@C_{20}H_{20}$ complex reveals that the He pair has a slightly stabilizing electrostatic interaction with the cage, which arises from an attraction between the electrons of helium dimer and the nuclei of the C sites in cage. It is evident from our discussion of the dissociation energies that the destabilization of the $He_2@C_{20}H_{20}$ complex arises from steric (hard sphere) repulsion between the He_2 unit and the $C_{20}H_{20}$ cage.

Figure 6 depicts the HOMO and the LUMO of $He_2@C_{20}H_{20}$. The HOMO lies completely on the $C_{20}H_{20}$ cage, while the LUMO is mainly a strong He_2–cage antibonding contribution with a small He–He bonding contribution. This suggests that in the $He_2@C_{20}H_{20}$ anion or dianion, there

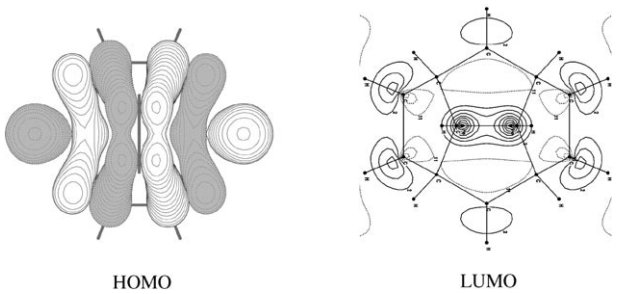

Figure 6. Isosurface of HOMO and contour line map of LUMO of D_{2h} $He_2@C_{20}H_{20}$ at B3LYP/def2-TZVPP.

would be a further reduction of the He–He distance by repulsion between the helium atom and the cage.

This prediction is confirmed by our B3LYP calculations,[38] which show a reduction of the He–He distance from 1.265 Å to 1.255 Å for the anion ($He_2@C_{20}H_{20}^-$) and to 1.244 Å for the dianion ($He_2@C_{20}H_{20}^{2-}$). Interestingly, the partial charge of the He atoms in both the anion and dianion is only +0.05. So the shortening of the He_2 distance is a consequence of a substantial He–cage repulsion, unaccompanied by any meaningful reduction in charge density of the antibonding σ_u He_2 molecular orbital to the cage.

Conclusion

The confinement of a pair of He atoms into the $C_{20}H_{20}$ cage leads to a high-energy distorted cage system in which the He–He separation is 1.265 Å, a separation that is less than half the He–He distance in He_2. The energy difference between the possible isomers is negligible (less than 0.15 kcal mol^{-1}), indicating that there is a nearly free precession movement of diatomic He_2 around its midpoint in the cage. Given the highly repulsive nature of the He–He and He–cage interactions and the small cavity size in $C_{20}H_{20}$, it would be difficult to synthesize the complex. Nonetheless, we consider that a study of inclusion complexes, such as the case we have selected and other systems that involve *artificially* compressed molecular fragments, are useful reference point in testing and extending our understanding of the bonding capabilities of otherwise unreactive or unstable species. The analysis of the bonding in endohedral (confinement) complexes, such as $He_2@C_{20}H_{20}$ is a vivid demonstration that a short internuclear separation does not necessarily imply the existence of a chemical bond. All bonding indicators we have considered, except the Bader analysis, show the absence of a genuine chemical bond. The high ionization energy of the He atom and the relatively low electron affinity of $C_{20}H_{20}$ explain the small electron transfer between the He atom and the cage. A comparison of $He_2@C_{20}H_{20}$ with $Xe_2@C_{60}$ is instructive. In both systems the free Ng–Ng distance is shortened as a consequence of the cage confinement. However, although a significant degree of bonding is obtained between the Xe atoms $Xe_2@C_{60}$, the helium atoms in the $He_2@C_{20}H_{20}$ complex show no tendency towards bond formation, even though the He atoms are rather close to each other at 1.265 Å in $C_{20}H_{20}$. We are interested in exploring further the electronic interaction of He and other inert chemical species in molecular cavities that afford even more significant restrictions in motion and spatial confinement and in cages with an increased Lewis acidity compared to the C_{60} or $C_{20}H_{20}$ frameworks. Steps in these directions are in progress.

Acknowledgements

We gratefully acknowledge support from Concyteg (Grant UGTO-PTC-079) and Conacyt (Grant 47175). A.K. acknowledges support from the Norwegian Research Council through the CeO Centre for Theoretical and Computational Chemistry (Grant No. 179568V30). K.J.D. thanks the University of Richmond for funding; the Arts and Sciences Faculty Research Committee is gratefully acknowledged for the award of a Summer Fellowship. E.C. acknowledges Conacyt and Concyteg for the Ph.D. fellowship. R.F. acknowledges Conacyt for the postdoctoral fellowship.

[1] J. C. Slater, *Phys. Rev.* **1928**, *32*, 349.
[2] F. Luo, C. F. Giese, W. R. Gentry, *J. Chem. Phys.* **1996**, *104*, 1151.
[3] W. Schöllkopf, J. P. Toennies, *J. Chem. Phys.* **1996**, *104*, 1155.
[4] T. J. Giese, D. M. York, *Int. J. Quantum Chem.* **2004**, *98*, 388.
[5] L. L. Lohr, S. M. Blinder, *J. Chem. Educ.* **2007**, *84*, 860.
[6] F. Grandinetti, *Int. J. Mass Spectrom.* **2004**, *237*, 243.
[7] L. Pauling, *J. Chem. Phys.* **1933**, *1*, 56.
[8] T. Peres, B. P. Cao, W. D. Cui, A. Khong, R. J. Cross, M. Saunders, C. Lifshitz, *Int. J. Mass Spectrom.* **2001**, *210*, 241.
[9] A. Khong, H. A. Jimenez-Vazquez, M. Saunders, R. J. Cross, J. Laskin, T. Peres, C. Lifshitz, R. Strongin, A. B. Smith, *J. Am. Chem. Soc.* **1998**, *120*, 6380.
[10] J. Laskin, T. Peres, C. Lifshitz, M. Saunders, R. J. Cross, A. Khong, *Chem. Phys. Lett.* **1998**, *285*, 7.
[11] A. Krapp, G. Frenking, *Chem. Eur. J.* **2007**, *13*, 8256.
[12] H. A. Jimenez-Vazquez, J. Tamariz, R. J. Cross, *J. Phys. Chem. A* **2001**, *105*, 1315.
[13] R. J. Cross, M. Saunders, H. Prinzbach, *Org. Lett.* **1999**, *1*, 1479.
[14] S. F. Boys, F. Bernardi, *Mol. Phys.* **1970**, *19*, 553.
[15] F. M. Bickelhaupt, E. J. Baerends in *Reviews in Computational Chemistry, Vol. 15* (Eds.: K. B. Lipkowitz, D. B. Boyd), Wiley, New York, **2000**.
[16] G. te Velde, F. M. Bickelhaupt, E. J. Baerends, C. F. Guerra, S. J. A. Van Gisbergen, J. G. Snijders, T. Ziegler, *J. Comput. Chem.* **2001**, *22*, 931.
[17] K. Kitaura, K. Morokuma, *Int. J. Quantum Chem.* **1976**, *10*, 325.
[18] A. D. Becke, *Phys. Rev. A* **1988**, *38*, 3098.
[19] J. P. Perdew, *Phys. Rev. B* **1986**, *33*, 8822.
[20] R. F. W. Bader, *Atoms in Molecules. A Quantum Theory*, Oxford University Press, Oxford, **1990**.
[21] K. B. Wiberg, *Tetrahedron* **1968**, *24*, 1083.
[22] R. F. W. Bader, *J. Phys. Chem. A* **1998**, *102*, 7314.
[23] F. Biegler-KÖnig, J. SchÖnbohm, *J. Comput. Chem.* **2002**, *23*, 1489.
[24] F. Biegler-König, J. SchÖnbohm, D. Bayles, *J. Comput. Chem.* **2001**, *22*, 545.
[25] Gaussian 03 (Revision D.02), M. J. Frisch, G. W. Trucks, H. B. Schlegel, G. E. Scuseria, M. A. Robb, J. R. Cheeseman, J. A. Montgomery, Jr., T. Vreven, K. N. Kudin, J. C. Burant, J. M. Millam, S. S. Iyengar, J. Tomasi, V. Barone, B. Mennucci, M. Cossi, G. Scalmani, N. Rega, G. A. Petersson, H. Nakatsuji, M. Hada, M. Ehara, K. Toyota, R. Fukuda, J. Hasegawa, M. Ishida, T. Nakajima, Y. Honda, O. Kitao, H. Nakai, M. Klene, X. Li, J. E. Knox, H. P. Hratchian, J. B. Cross, C. Adamo, J. Jaramillo, R. Gomperts, R. E. Stratmann, O. Yazyev, A. J. Austin, R. Cammi, C. Pomelli, J. W. Ochterski, P. Y. Ayala, K. Morokuma, G. A. Voth, P. Salvador, J. J. Dannenberg, V. G. Zakrzewski, S. Dapprich, A. D. Daniels, M. C. Strain, O. Farkas, D. K. Malick, A. D. Rabuck, K. Raghavachari, J. B. Foresman, J. V. Ortiz, Q. Cui, A. G. Baboul, S. Clifford, J. Cioslowski, B. B. Stefanov, G. Liu, A. Liashenko, P. Piskorz, I. Komaromi, R. L. Martin, D. J. Fox, T. Keith, M. A. Al-Laham, C. Y. Peng, A. Nanayakkara, M. Challacombe, P. M. W. Gill, B. Johnson, W. Chen, M. W. Wong, C. Gonzalez, J. A. Pople, Gaussian, Inc., Pittsburgh, PA, **2004**.
[26] E. Cerpa, A. Krapp, A. Vela, G. Merino, *Chem. Eur. J.* **2008**, *14*, 10232.
[27] M. J. Feinberg, K. Ruedenberg, *J. Chem. Phys.* **1971**, *54*, 1495.

[28] A. Haaland, D. J. Shorokhov, N. V. Tverdova, *Chem. Eur. J.* **2004**, *10*, 4416.
[29] J. Poater, M. Sola, F. M. Bickelhaupt, *Chem. Eur. J.* **2006**, *12*, 2889.
[30] J. Poater, R. Visser, M. Sola, F. M. Bickelhaupt, *J. Org. Chem.* **2007**, *72*, 1134.
[31] A. E. Reed, L. A. Curtiss, F. Weinhold, *Chem. Rev.* **1988**, *88*, 899.
[32] A. D. Becke, *J. Chem. Phys.* **1993**, *98*, 5648.
[33] C. T. Lee, W. T. Yang, R. G. Parr, *Phys. Rev. B* **1988**, *37*, 785.
[34] F. Weigend, R. Ahlrichs, *Phys. Chem. Chem. Phys.* **2005**, *7*, 3297.
[35] C. Møller, M. S. Plesset, *Phys. Rev.* **1934**, *46*, 618.
[36] F. Weigend, M. Haser, H. Patzelt, R. Ahlrichs, *Chem. Phys. Lett.* **1998**, *294*, 143.
[37] R. Ahlrichs, M. Bar, M. Haser, H. Horn, C. Kolmel, *Chem. Phys. Lett.* **1989**, *162*, 165.
[38] These calculations were done with the B3LYP/6-311G(d,p) level in Gaussian 03.

Received: July 10, 2008
Published online: November 19, 2008

